Chinese Chemical Letters 34 (2023) 107917

Contents lists available at ScienceDirect

Chinese Chemical Letters

journal homepage: www.elsevier.com/locate/cclet

Superhigh intrinsic proton conductivity in densely carboxylic covalent organic framework

Jinli Li, Junhua Wang, Feng Shui, Mao Yi, Zhiyuan Zhang, Xiongli Liu, Laiyu Zhang, Zifeng You, Rufeng Yang, Shiqi Yang, Baiyan Li*, Xian-He Bu

School of Materials Science and Engineering, National Institute for Advanced Materials, TKL of Metal and Molecule-Based Material Chemistry, Nankai University, Tianjin 300350, China

ARTICLE INFO

Article history:
Received 1 September 2022
Revised 28 September 2022
Accepted 17 October 2022
Available online 19 October 2022

Keywords:
Covalent organic frameworks (COFs)
Pre-assembly approach
Intrinsic proton conductivity
Rational design
Carboxylic acid

ABSTRACT

Herein, we developed for the first time two carboxylic acid based intrinsic proton conductors (COOH-COF-1 and COOH-COF-2) *via* pre-assembly approach. The obtained COOH-COF-1 and COOH-COF-2 not only show outstanding chemical and thermal stabilities, but also exhibit superhigh intrinsic proton conductive behaviors. Especially, the intrinsic proton conductivity of COOH-COF-2 is up to 2.6×10^{-3} S/cm at 353 K and 98% RH, which is the highest value among all the reported acid functionalized COFs. This work lights up the way for the rational design of functional COFs with remarkably intrinsic proton conducting performance and related practical applications.

As the key component of proton exchange membrane fuel cells (PEMFCs), proton conductive materials play a vital role in the application and manufacture of PEMFCs. Currently, developing proton conducting materials with both high stability and excellent proton conductivity is highly desired [1–4]. Nafion, as the most widely used proton conductive materials, can afford high proton conductivity and maintain long working life in PEMFCs. However, the high-cost preparation, complicated process, and restricted operating conditions impede its further applications [5,6]. Moreover, the amorphous structure makes it difficult to thoroughly understand the relationship between structure and property [7].

Recently, covalent organic frameworks (COFs) emerging as new crystalline materials, have gathered tremendous interest and been applied in diverse applications, such as gas storage and separation, drug delivery and catalysis [7–13]. COFs are constructed by light elements (B, C, N, O) *via* covalent bonds with relatively lightweight, exhibit superhigh thermal and chemical stability, and possess membrane processability [3,14–16]. These prominent features of COFs render a promising platform for intrinsic proton conduction. In 2014, Banerjee and co-workers firstly developed H_3PO_4@Tp-Azo as a proton conductor [17]. However, its proton conductivity is only 9.9×10^{-4} S/cm under hydrous state. Subsequently, extensive efforts have been made to enhance proton conductivity [18–23]. The convenient and universal strategy for constructing proton conductive COFs still relies on loading guest molecules as proton sources. Such approach would inevitably lead to the leakage of proton carriers and unstable proton conductive performance, thereby impeding their practical applications. Hence, it is still a necessary and urgent task to develop COFs with intrinsic proton conductivity, effectively ensuring stable proton conductive performance. Up to now, sorts of functionalized COFs have shown excellently intrinsic proton conduction with sulfonic acid [19,24–27], phosphorous acid [28], imidazole [29], and phenolic hydroxyl in the skeleton [30]. However, only limited example employed carboxylic groups as proton carrier to construct intrinsic proton conductive COFs *via* post-synthetic modification (PSM) process under harsh conditions [31]. In this regard, the PSM method would be difficult to convert all precursor groups completely into carboxylic groups, which would inevitably affect the array of proton carriers and proton conductive performance. In addition, such PSM approach can only be applied to limited ultrastable COFs due to the potential decomposition of most COFs under violent hydrolysis conditions [31].

Herein, in this context, we aimed to develop such carboxylic COF with high proton conductivity *via* pre-assembly approach based on the following design principles (Fig. 1): (1) selecting building blocks with a large amount of carboxylic groups for constructing carboxylic acid functionalized COF *via* pre-assembly approach, that effectively avoids the problems caused by post-modification synthesis such as incomplete hydrolysis and discon-

* Corresponding author.
E-mail address: libaiyan@nankai.edu.cn (B. Li).

https://doi.org/10.1016/j.cclet.2022.107917
1001-8417/

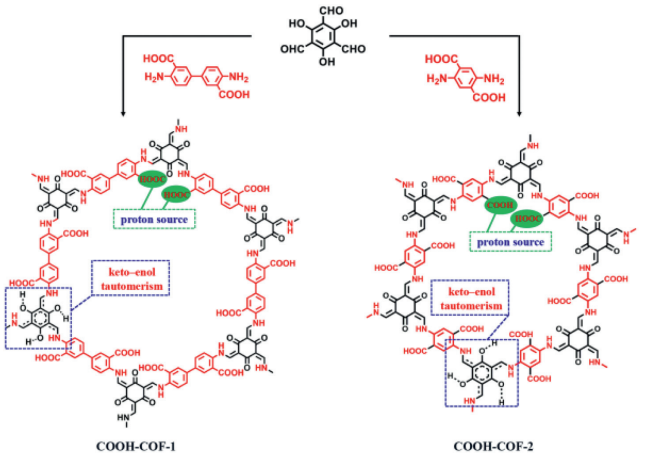

Fig. 1. The synthesis and design principle of COOH-COF-1 and COOH-COF-2 and the proton source in them.

tinuous proton distribution in the pores; (2) achieving suitable pore size for accelerating the mass transfer of proton [32]; (3) decorating highly dense carboxylic groups on the framework can not only serve as an intrinsic proton source, but also provide an endless array of proton-conducting sites, thereby endowing the possibility of intrinsic proton conduction [31,33]; (4) obtaining highly stable framework by keto-enol tautomerism for promising applications under harsh conditions [34]; (5) long-range ordered 1D channels accelerate proton movement [33,35].

Considering all these factors, two optimized carboxylic acid COFs, namely COOH-COF-1 and COOH-COF-2, were synthesized by 1,3,5-triformylphloroglucinol (TP) with 4,4′-diaminobiphenyl-3,3′-dicarboxylic acid (DBA) or 2,5-diaminoterephthalic acid (H_2DATA) based on reversible Schiff base reaction [8,36]. The obtained COOH-COF-1 and COOH-COF-2 not only exhibit superior chemical (organic solvent and water) and thermal (~300 °C) stabilities, but also show outstanding intrinsic proton conductivity (1.4×10^{-3} and 2.6×10^{-3} S/cm) under hydrous state, which is the highest value among all acidic group functionalized COFs reported to date, such as GS-COF-1-COOH [31], GS-COF-2-COOH [31], TFPPY-PDA-COF-H_2PO_3 [28] and NKCOF-26 [21]. This work thus lights up the road to rational design of functional COFs with outstanding intrinsic proton conductive performance.

The crystallinity of COOH-COF-1 and COOH-COF-2 is confirmed by powder X-ray diffraction (PXRD) measurement. The PXRD of COOH-COF-1 illustrated two prominent peaks at about 3.4°, 6.1° and several weak peaks at higher angles, matching well with the PXRD pattern of the simulated AA packing structure (Fig. 2a) [36]. Likewise, COOH-COF-2 showed one prominent peak at about 4.8°, several indistinct peaks at higher angles, which is consistent with the PXRD pattern of the simulated AA packing structure (Fig. 2b).

The successful formation of COOH-COF-1 and COOH-COF-2 was further confirmed by Fourier transform infrared (FT-IR) spectroscopy, X-ray photoelectron spectroscopy (XPS) and solid-state ^{13}C nuclear magnetic resonance (NMR) technologies. FT-IR spectroscopy of COOH-COF-1 and COOH-COF-2 revealed the complete consumption of reactants by the disappearance of aldehydic −CH=O (1650 cm^{-1}) in TP monomer, and the N−H stretching bands (3335–3058 cm^{-1}) of free diamine (Figs. 2c and d). Meanwhile, new characteristic stretching bands arose at 1696 (C=O), 1574 (C=C), and 1230 cm^{-1} (C−N), indicating the successful formation of keto-form structure in COOH-COF-1 and COOH-COF-2 [37]. This result was further confirmed by the results of ^{13}C NMR spectrum of COOH-COF-1 and COOH-COF-2, in which peaks at about 182.3 ppm, 144.8 ppm and 107.3 ppm, were attributed to C=O, C−N and C=C bonds (Fig. S2 in Supporting information) [17,38,39]. In addition, the florescence of COOH-COF-1 and COOH-COF-2 was quenched with decreasing pH value, which further illustrate the formation of imine bond (Fig. S3 in Supporting information) [40,41]. Moreover, the peaks located at about 533.2 and 532.3 eV in O 1s XPS spectrum can be attributed to the oxygen atoms in carboxylic groups (Figs. S4b and S5b in Supporting information), indicated the successful synthesis of COOH-COF-1 and COOH-COF-2 [37].

The porosity of COOH-COF-1 and COOH-COF-2 was revealed by N_2 adsorption at 77 K. Both the adsorption curves of COOH-COF-1 and COOH-COF-2 showed a steep uptake at the high-pressure region ($P/P_0 > 0.8$), which corresponded well with the type II sorption model. The Brunauer-Emmett-Teller (BET) surface areas of COOH-COF-1 and COOH-COF-2 were 227.6 and 117.2 m^2/g (Fig. S6 in Supporting information), respectively. And their pore sizes were calculated to be 1.7 and 1.1 nm (Fig. S7 in Supporting information), respectively, which is slightly lower than that obtained from the simulated structures. This may due to the extrusion deformation caused by abundant carboxylic acid groups in the skeleton. Thermogravimetric analysis (TGA) demonstrated that the thermal stability of COOH-COF-1 and COOH-COF-2 were up to 300 °C under N_2 atmosphere (Fig. S8 in Supporting information), which can guarantee the practical requirement under wide temperature range. Furthermore, the PXRD patterns of COOH-COF-1 and COOH-COF-2 showed almost on change before and after immersion in DMF, water, 2 mol/L HCl, 3 mol/L NaCl and 3 mol/L $NaHCO_3$ for 12 h (Fig. 3 and Fig. S9 in Supporting information), suggesting their excellent chemical stabilities and insolubilities.

Considering superior chemical and thermal stabilities, and the abundant carboxylic groups as proton carries in the framework, we utilized them as pristine proton conductors. Electrochemical impedance spectroscopy (EIS) measurement was applied to investigate the proton conductivity. As illustrated in Fig. S10 (Supporting information), COOH-COF-1 and COOH-COF-2 showed negligible proton conductivity under anhydrous conditions. However, under 98% relative humidity (RH) condition, the proton conductivity of COOH-COF-1 and COOH-COF-2 increased dramatically from 298 to 353 K (Figs. 4a and b). This phenomenon indicates the key role of water molecules in proton movement, which is well consistent with previous reports [24,42]. Under 98% RH, the proton conductivity of COOH-COF-1 varied from 1.5×10^{-4} S/cm to 1.4×10^{-3} S/cm during the temperature range of 298–353 K (Fig. 4a). In addition, the proton conductivity of COOH-COF-2 (Fig. 4b) was up to 2.6×10^{-3} S/cm (353 K and 98 %RH), which is the highest value among all intrinsic proton conductive COFs with proton acid sites (GS-COF-2-COOH [31], GS-COF-1-COOH [31], TFPPY-PDA-COF-H_2PO_3 [28], NKCOF-26 [21], NKCOF-3 [38], TFPPY-BT-COF-H_2PO_3 [28], NKCOF-27 [21], aza-COF-1 [43] and aza-COF-2 [43]), second to the highest imidazole-based COF (BIP) [29], ranking it as among the best COF-based intrinsic proton conductive materials (Fig. 4c). And the *Ea* value of COOH-COF-1 and COOH-COF-2 are calculated to be 0.38 eV and 0.23 eV (Fig. S11 in Supporting information), involving the "Grotthuss mechanism" (< 0.40 eV) in proton migration. Compared with COOH-COF-1, COOH-COF-2 exhibit higher proton conductivity and lower E_a value, which may be attributed to the higher density of carboxylic groups and H-bond networks in the framework [33,35].

To further investigate the crucial role of carboxylic groups in proton conduction, an analogous COF (namely TPBD, without carboxylic groups in the framework compared to COOH-COF-1) was synthesized by reacting TP and benzidine as control experiment (Fig. S12 in Supporting information). TPBD only showed proton conductivity of 8.7×10^{-5} S/cm under identical conditions (353 K and 98% RH) (Fig. S13 in Supporting information), which is two orders of magnitude lower than that of COOH-COF-1. This result thus illustrated the introduction of large amounts of carboxylic sites

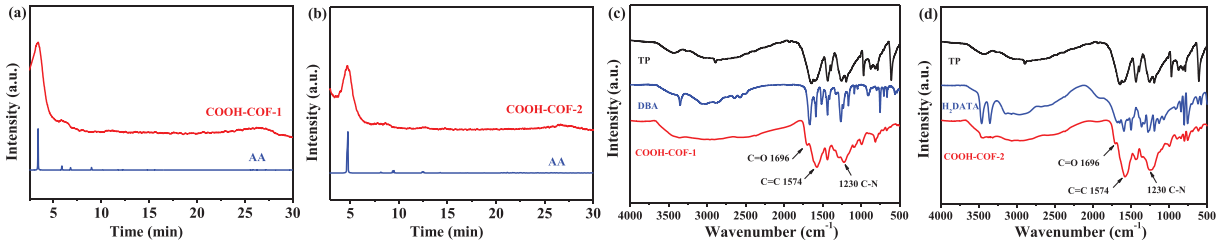

Fig. 2. The experimental and simulated (AA stacking) PXRD patterns of (a) COOH-COF-1 and (b) COOH-COF-2, respectively; FI-IR spectra of (c) COOH-COF-1, (d) COOH-COF-2, and starting materials.

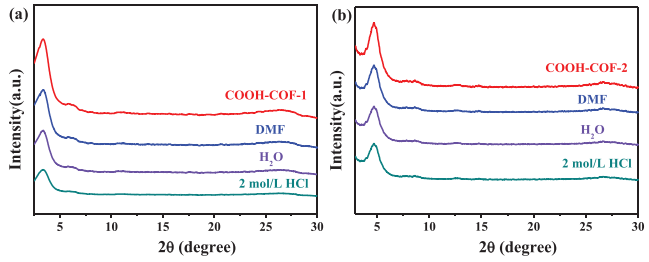

Fig. 3. The PXRD patterns of (a) COOH-COF-1 and (b) COOH-COF-2 after treating with DMF, H_2O and 2 mol/L HCl for 12 h.

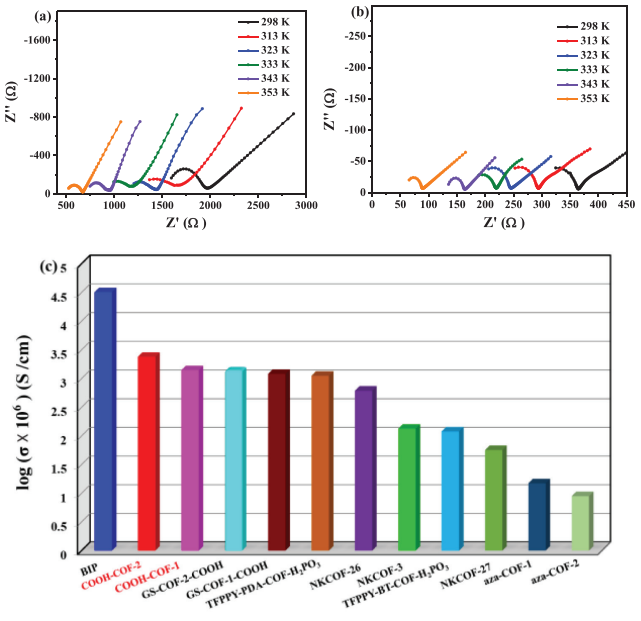

Fig. 4. Nyquist plots of (a) COOH-COF-1 and (b) COOH-COF-2 under 98% RH at different temperatures; (c) comparing the intrinsic proton conductivity of COOH-COF-1 and COOH-COF-2 with COF-based benchmarked proton conductors under humid conditions, including BIP [29], GS-COF-2-COOH [31], GS-COF-1-COOH [31], TFPPY-PDA-COF-H_2PO_3 [28], NKCOF-26 [21], NKCOF-3 [38], TFPPY-BT-COF-H_2PO_3 [28], NKCOF-27 [21], aza-COF-1 [43], and aza-COF-2 [43].

into COFs contribute to their high proton conductivities. Furthermore, we also measured the proton conductivity of COOH-COF-1 with different particle sizes under the same conditions. The results show that smaller particle size is beneficial for the higher proton conductivity, which may due to the more compact packing, higher proton concentration, denser hydrogen bond network, and shorter proton transport distance under the same experimental conditions (Fig. S14 in Supporting information) [21].

In summary, we have successfully designed and synthesized two high-densely carboxylic acid functionalized COFs, COOH-COF-1 and COOH-COF-2. They not only exhibited high chemical and thermal stabilities but also showed superhigh intrinsic conductive behaviors. Especially, the intrinsic proton conductivity of COOH-COF-2 is up to 2.6×10^{-3} S/cm at 353 K and 98% RH, which is the highest value among all the reported acid functionalized COFs. This work lights up the way for the rational design of functional COFs with exceptional intrinsic proton conducting performance and related practical applications.

Declaration of competing interest

The authors declare no conflict of interest.

Acknowledgments

This work was supported by the National Natural Science Foundation of China (Nos. 21978138 and 22035003), the Fundamental Research Funds for the Central Universities (Nankai University), and the Haihe Laboratory of Sustainable Chemical Transformations (No. YYJC202101).

Supplementary materials

Supplementary material associated with this article can be found, in the online version, at doi:10.1016/j.cclet.2022.107917.

References

[1] W. Gao, G. Wu, M.T. Janicke, et al., Angew. Chem. Int. Ed. 53 (2014) 3588–3593.
[2] Y. Yang, P. Zhang, L. Hao, et al., Angew. Chem. Int. Ed. 60 (2021) 21838–21845.
[3] Z.C. Guo, Z.Q. Shi, X.Y. Wang, Z.F. Li, G. Li, Coord. Chem. Rev. 422 (2020) 213465.
[4] X. Meng, H.N. Wang, S.Y. Song, HJ. Zhang, Chem. Rev. 46 (2017) 464–480.
[5] K.A. Mauritz, R.B. Moore, Chem. Rev. 104 (2004) 4535–4585.
[6] A. Kraytsberg, Y. Ein-Eli, Energy Fuels 28 (2014) 7303–7330.
[7] E.B. Trigg, T.W. Gaines, M. Maréchal, et al., Nat. Chem. 17 (2018) 725–731.
[8] Y. Zhao, G. Guo, J. Zhao, Patent, CN113788937A.
[9] P. She, Y. Qin, X. Wang, Q. Zhang, Adv. Mater. 34 (2022) 2101175.
[10] Y. Li, W. Chen, G. Xing, D. Jiang, L. Chen, Chem. Soc. Rev. 49 (2020) 2852–2868.
[11] M.X. Wu, Y.W. Yang, Chin. Chem. Lett. 28 (2017) 1135–1143.
[12] N. Liu, L. Shi, X. Han, Z.Q. Wu, X. Zhao, Chin. Chem. Lett. 31 (2020) 386–390.
[13] H. Wang, H. Ding, X. Meng, C. Wang, Chin. Chem. Lett. 27 (2016) 1376–1382.
[14] F. Yu, W. Liu, S.W. Ke, M. Kurmoo, J.L. Zuo, et al., Nat. Commun. 11 (2020) 5534.
[15] X. Zhao, Y. Chen, Z. Wang, Z. Zhang, Polym. Chem. 12 (2021) 4874–4894.
[16] F. Yu, W. Liu, B. Li, et al., Angew. Chem. Int. Ed. 58 (2019) 16101–16104.
[17] S. Chandra, T. Kundu, S. Kandambeth, et al., J. Am. Chem. Soc. 136 (2014) 6570–6573.
[18] M. Di, L. Hu, L. Gao, et al., Chem. Eng. J. 399 (2020) 125833.
[19] L. Cao, H. Wu, Y. Cao, et al., Adv. Mater. 32 (2020) 2005565.
[20] C. Yang, L. Hou, J. Zhao, et al., Chem. Eng. J. 428 (2022) 131124.
[21] S. Jia, P. Zhao, Q. Liu, et al., Chem. Res. Chin. Univ. 38 (2022) 461–467.
[22] S. Bian, K. Zhang, Y. Wang, et al., ACS Appl. Energy Mater. 5 (2022) 1298–1304.
[23] Y. Fu, Y. Wu, S. Chen, et al., ACS Nano 15 (2021) 19743–19755.
[24] Y. Peng, G. Xu, Z. Hu, et al., ACS Appl. Mater. Interfaces 8 (2016) 18505–18512.
[25] P. Li, J. Chen, S. Tang, Chem. Eng. J. 415 (2021) 129021.
[26] S. Chandra, T. Kundu, K. Dey, et al., Chem. Mater. 28 (2016) 1489–1494.
[27] L. Zhai, Y. Yao, B. Ma, et al., Macromol. Rapid Commun. 43 (2022) 2100590.
[28] Z. Lu, C. Yang, L. He, et al., J. Am. Chem. Soc. 144 (2022) 9624–9633.
[29] K.C. Ranjeesh, R. Ilathvalappil, S.D. Veer, et al., J. Am. Chem. Soc. 141 (2019) 14950–14954.
[30] J. Li, J. Wang, Z. Wu, S. Tao, D. Jiang, Angew. Chem. Int. Ed. 60 (2021) 12918–12923.
[31] Y. Su, Y. Wan, H. Xu, et al., J. Am. Chem. Soc. 142 (2020) 13316–13321.

[32] P. Wang, Q. Xu, Z. Li, et al., Adv. Mater. 30 (2018) 180199.
[33] C. Maffeo, S. Bhattacharya, J. Yoo, D. Wells, A. Aksimentiev, Chem. Rev. 112 (2012) 6250–6284.
[34] S. Kandambeth, A. Mallick, B. Lukose, et al., J. Am. Chem. Soc. 134 (2012) 19524–19527.
[35] H. Xu, S. Tao, D. Jiang, Nat. Chem. 15 (2016) 722–726.
[36] J.Y. Yue, L. Wang, Y. Ma, et al., Dalton Trans. 48 (2019) 17763–17769.
[37] B. Dong, W.J. Wang, S.C. Xi, D.Y. Wang, R. Wang, Chem. Eur. J. 27 (2021) 2692–2698.
[38] Y. Yang, X. He, P. Zhang, et al., Angew. Chem. Int. Ed. 59 (2020) 3678–3684.
[39] K. Jeong, S. Park, G.Y. Jung, et al., J. Am. Chem. Soc. 141 (2019) 5880–5885.
[40] Z. Li, Z. Yang, Y. Zhang, B. Yang, Y.W. Yang, Angew. Chem. Int. Ed. 61 (2022) e202206144.
[41] L. Ascherl, E.W. Evans, J. Gorman, et al., J. Am. Chem. Soc. 141 (2019) 15693–15699.
[42] L. Liu, L. Yin, D. Cheng, et al., Angew. Chem. Int. Ed. 60 (2021) 14875–14880.
[43] Z. Meng, A. Aykanat, K.A. Mirica, Chem. Mater. 31 (2019) 819–825.